

NephroProt: Diagnostic test based on a Two Component System (TSC), for the detection of biomarkers present in early stages of Diabetic Nephropathy

Centeno Noriega Ana Sofía, Gallegos Solís Lorena, Giles Buzo Gabriela, Bautista Novoa Brenda, Briseño-Bautista Adalberto, MirandaTrejo Tania Fernanda, Makoszay-Castañón Santiago, Rojas Amador Valeria, Matínez Romérom Ana Paula, Alonso Juárez Ariadna, Ortega Delgado Ximena, Torres Huerta Ana Laura, Antonio Pérez Aurora

Introduction

Diabetes is a growing global health challenge, which is the 9th leading cause of death in the United States (Reichel, 2022) and affects over 62 million people in the Americas, a number expected to rise to 109 million by 2040 (OPS, 2021). In Mexico, diabetes is one of the diseases with more incidence and mortality, being the second major cause of death. In 2021, 12.4 million people suffered from diabetes, Type 2 being the most common among people over 60 years, although it can occur at any age (Secretaría de Salud, 2022).

Unfortunately, both types of diabetes can trigger a series of subsequent pathologies and complications that ultimately reduce the life quality of patients, since it is the leading cause of chronic kidney disease (CKD) and end-stage kidney disease (ESKD) worldwide (Hoogeveen, 2022). Among such complications, we can find diabetic nephropathy (DN), which is a major concern since it is estimated that 1 in every 3 diabetics develop DN (NIH, 2017) and every 24 hours, 170 people with diabetes begin treatment for kidney failure (CDC, 2022). Particularly in Mexico, in 2021 alone, 6.2 million new patients were diagnosed with diabetic nephropathy and it is estimated that 20-40% of patients with diabetes Type 2 and 15% of patients with diabetes Type 1 will suffer from diabetic nephropathy (Fuentes *et al.*, 2022).

Diabetic nephropathy

When the kidneys are damaged, they can not filter the blood correctly, contaminants and waste build-up, and major health issues develop. Diabetic kidney disease (DKD), also known as diabetic nephropathy, is the most common cause of ESKD (Varghese & Jialal, 2023). A microangiopathic complication, that contributes to impairments in the kidney filtering system, can lead to the final condition of renal failure (De los Ríos Castillo *et al.*, 2005). Kidney damage caused by diabetes usually occurs slowly over many years and most people with DKD show no symptoms (NIH, 2017). DN leads to loss of kidney function and is the main cause of CKD. The classification of the different stages in DN (**Table 1**) is based on the percentage of renal function, which is measured through an indicator of effective kidney function: glomerular filtration rate (GFR).

Table 1. Diabetic Nephropathy stages according to the percentage of renal function.

Stage	Renal function (% GFR)
1	90-100
2	60-98
3	30-59
4	15-29
5	<15

The pathogenesis of the disease is initiated and maintained by 4 types of conditions: metabolic, hemodynamic, growth, and profibrotic and proinflammatory factors. Metabolic factors are mainly caused by alterations in tissues due to products of glucose metabolism in hyperglycemia. At the same time, advanced glycation end products (AGEs) are produced and activate receptor cells, which generates reactive oxygen species (ROS) and ultimately leads to oxidative stress. As for the hemodynamic factors, the increment of glomerular capillary pressure increases the Nerve Growth Factor Receptor (NGFR), causing hyperfiltration. Regarding growth factors, the vascular endothelial growth factor (VEGF) causes vascular expansion, which leads to hyaline arteriosclerosis and hypertension changes in the kidney. Finally, the profibrotic factors and proinflammatory factors are the main cause of tubular fibrosis and the progress of DN by macrophages infiltration (Argawal, 2021).

Relevance of early diagnosis and current methods for detecting DN

Being DN the leading cause of end-stage renal disease worldwide, diagnosis of patients prone to develop DN, is critical for reducing DN prevalence, retarding its progression (Thipsawat, 2021) and avoiding a significant decrease in life expectancy (Bosan, 2007). Additionally, early diagnosis is critical because, as shown in **Table 1**, renal function continues decreasing as the patient advances towards the last stage (stage 5).

Moreover, the study of Thornton-Snyder *et al.* (2019) provides an insight of the health and economic benefits of earlier diagnosis and treatment of DKD, by identifying at-risk patients with a cost-effective biomarker test. Their modeling results for a prognostic biomarker test indicate

that, compared to baseline, the prevalence of DKD declined 5.1%, the prevalence of diabetes with stage 5 CKD declined 3.0%, people with diabetes gained 0.2 years in life expectancy, and per-capita annual medical spending fell by 0.3%. This prediction supports the positive impact of an early-diagnostic test for DN on the patients' quality of life and economy.

While current tests for detecting kidney damage exist, based mainly on biomarkers from blood and urine (Mizdrak *et al.*, 2022), they exhibit a significant drawback: they identify damage at advanced stages. Some examples are late-stage biomarkers such as albumin and creatinine, which can be measured until there is significant kidney damage, limiting timely treatment (De los Ríos Castillo *et al.*, 2005). Particularly, tests that rely on albumin have a threshold set at concentrations greater than 30 mg/24h (Fierro *et al.*, 2010). Regrettably, this means the detection of DN occurs at the third or fourth stage, characterized by substantial renal function impairment, as presented in **Table 1**.

Biomarkers

As mentioned previously, the biomarkers measured in the actual diagnostic methods are considered late-stage biomarkers. Thus, specific biomarkers of diabetic nephropathy that are present in the early stages of the disease were investigated. In this sense, a deep research in different sources was carried out for different biomarkers related to DN (**Figure 1**). After such review, advantages and disadvantages of the biomarkers were compared (see example in **Table 2**) as well as the selection criteria met (see example in **Table 3**). The final candidates for the proposal were: Neutrophil Associated Lipocalin (NGAL) and Transferrin (serotransferrin being its most common isoform in urine).

	Advantages	Disadvantages
Cystatin C	Protein mainly used as a kidney function marker. When blood levels of cystatin C rise, it's an indicator that kidney function and GFR decline (Chen <i>et al.</i> , 2017). This biomarker is less dependent on age, sex, and weight for measuring kidney function than creatinine (Lisak & Lopez, 2018)	It has also been observed to be an experimental biomarker for cardiovascular and neurodegenerative diseases (Chen <i>et al.</i> , 2017).
Alpha-1-microglobulin (A1M)	Biomarker for differentiating between patients with Type 2 diabetes (0.84 ± 0.5 g/24 hrs) and patients with no diabetes history (0.16 ± 0.12 g/24 hrs) (Shore <i>et al.</i> , 2019).	Might not be a specific biomarker for distinguishing between individuals with kidney damage (microalbuminuria) and those with normal kidney function (normoalbuminuria) (Shore <i>et al.</i> , 2019).
8-oxodG and 8-oxodG	the amount in urine of 8-oxodG with DN is greater than in healthy patients. Specifically, diabetic D2 patients manifested increased mitochondrial DNA lesions (8-oxodG) exclusively located in glomerular endothelial cells after 3 weeks of diabetes, and these accumulated over time in addition to increased urine secretion of 8-oxo-deoxyguanosine. It's a good biomarker for oxidative stress in DN (Wu <i>et al.</i> , 2004).	Are most usually used to detect DNA lesions (Wu <i>et al.</i> , 2004).
FABP-1	With respect to diabetic nephropathy and acute kidney disease (AKI), urinary L-FABP is an early diagnostic of kidney disease or a predictive marker for renal prognosis. After many clinical studies, urinary L-FABP was approved as a new tubular biomarker promulgated by the Ministry of Health, Labour and Welfare in Japan (Chi <i>et al.</i> , 2019). There have been several studies where their results indicate that the α-FABP concentration is negatively proportional to the estimated glomerular filtration rate (eGFR), and has shown earlier shifts in concentration than albumin between diabetic patients with and without DN (Thu <i>et al.</i> , 2019).	Although is a molecule that has been related to kidney diseases, L-FABP is a mediator of lipid metabolism and has been associated with liver injury. Urinary L-FABP and MELD-Na were associated with 90-day mortality in patients with decompensated cirrhosis (Izumi <i>et al.</i> , 2022).
MCP-1/CCL2	Monocyte Chemoattractant Protein 1 (MCP-1), also known as CCL2, is a potent chemokine produced by renal cells and it has been shown that MCP-1 is overexpressed in the kidneys from diabetic animals. Contributes to kidney damage by monocyte renal cell recruitment and direct activation of resident renal cells (Tesch, 2006).	Since it is a molecule coming from an inflammatory response, it can be linked to other diseases (Tesch, 2006).
Type IV Collagen	The concentration increases in patients with normoalbuminuria and microalbuminuria compared with healthy patients and it is significantly related to the quantity of albuminuria (Moser, 2019)	A major disadvantage is that it has a massive number of glycosylation and hydroxylations, due to its necessary interactions between collagen chains (Moser, 2019)

Table 3. Comparison of selection criteria of the best biomarker candidates obtained from literature research.

Criteria	Cystatin C	A1M	NGAL	Transferrin	8-oxodG	Collagen Type IV	FABP-1	MCP-1/CCL2
Presence in urine in early and preventive stages of DN	X	X	✓	✓	X	X	✓	X
Specificity and/or not present in other diseases	X	X	✓	✓	X	X	X	X
Appearance independent of patients physiology	✓	X	✓	✓	X	X	X	X
Potential usage of bioreceptors for detection	X	X	✓	✓	X	X	X	X

Transferrin is a blood plasma glycoprotein that plays a central role in iron metabolism and is responsible for ferric-ion delivery. Transferrin functions as the most critical ferric pool in the body. It transports iron through the blood to various tissues, such as the liver, spleen, and bone marrow. It is an essential biochemical marker of body iron status (Ogun & Adeyinka, 2022). As a biomarker, it has been found that some patients with diabetes have high rates of transferrin excretion in the urine, which is related to the development of microalbuminuria (Lee & Choi, 2014). Microalbuminuria is basically the urinary excretion of albumin of 20 µg/minute to 200 µg/minute, and is a reliable predictor for diabetic nephropathy, and also serves to detect cardiovascular diseases in early stages in patients with diabetes (Majul & Camps, 2007). It is also considered the first sign of diabetic nephropathy (Terzic *et al.*, 2019). Likewise, Macroalbuminuria, also referred to as proteinuria, is defined as a protein excretion rate greater than 300 mg/day or greater than 200 µg/min (Kholza *et al.*, 2010).

The evolution of diabetic nephropathy has been associated with a gradual but considerable increase in urinary transferrin. According to a study, 95% of patients with microalbuminuria and 100% of patients with macroalbuminuria had increased urine transferrin excretion. The hypothesis that transferrin is a sensitive and particular marker for the identification of diabetic nephropathy is supported by these data (Khalid Al-Rubeaan *et al.*, 2017). On the other hand, NGAL is a protein involved in innate immunity by preventing iron usage by bacteria. It is

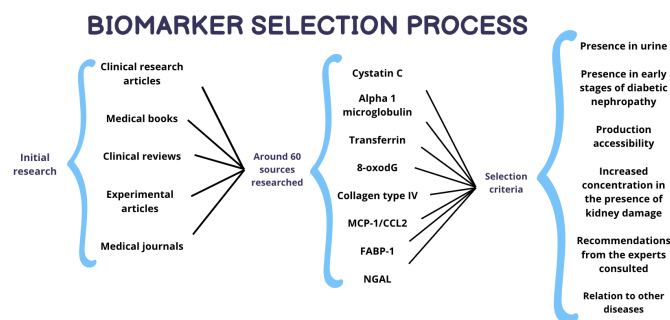


Figure 1. Diagram of the selection process followed for selecting the biomarkers with the most adequate characteristics for the design.

Table 2. Comparison of the advantages and disadvantages of cystatin C and A1M that were evaluated as selection criteria.

expressed in neutrophils and in low levels in the kidney, prostate and epithelia of the respiratory tract. In the case of acute kidney injury (AKI), NGAL is secreted in high levels into the blood and urine within 2 hours of injury. Because NGAL is protease resistant and small, it is easily excreted and detected in urine. NGAL can also be used as an early diagnosis for chronic kidney disease, contrast induced nephropathy, and kidney transplant (Goldstein, 2011).

Urinary NGAL appears to have a better diagnostic profile for acute kidney damage across diverse populations, it has a good diagnostic accuracy for cases of microalbuminuria, and a sufficient diagnostic accuracy for microalbuminuria (Khalid Al-Rubeaan *et al.*, 2017).

The presence of NGAL in certain concentrations indicate renal tubular damage, while Transferrin indicates renal glomerular damage.

The proposal

Due to the prevalence of DN in Mexico, as well as the lack of early diagnostic tests for DN and its implications (more complex patient prognosis, healthcare system, economic impact for the patient, and reduced life quality, among others), our aim is to innovate a simple, accessible, non-invasive and alternative diagnostic test for the diagnosis of DN in the early stages, to facilitate early detection and mitigating the progression of the disease. The proposal consists of a point-of-care diagnostic test grounded in a cell-free system integrated with a genetic circuit to detect the concentrations of significant and specific DN biomarkers in urine: neutrophil gelatinase-associated lipocalin (N-GAL) and serotransferrin. It is important to mention that the presence and contrast in the urine concentration of these biomarkers between diabetic patients with and without DN indicate renal affection (Campion *et al.*, 2017).

The detection system includes a chimeric protein formed by a proteic domain that undergoes autophosphorylation when a peptide interacts with a specific biomarker. The phosphate is then detected by an aspartate, which activates reporter genes through conformational changes ultimately allowing the identification of patients prone to develop DN. This approach is designed to detect the concentration of such biomarkers in urine, offering an insight of DN for early diagnosis and timely interventions, to reduce the risk of complications and improve life quality.

For the detection system, we proposed a laminar flow test, which is a widely used diagnostic technique that allows rapid and easy detection of a target analyte in a sample (Yuwei *et al.*, 2021).

Thus the test operates on the principle of capillary action, where the sample flows along a strip or porous membrane

by passive diffusion, the strip consists of different zones, each with a specific purpose, being the main ones the sample pad, the conjugate pad and the nitrocellulose membrane (Yuwei *et al.*, 2021).

The sample pad is where the sample is applied, usually via a liquid sample or sample collection device and it helps ensure uniform sample distribution throughout the test (Yuwei *et al.*, 2021).

The conjugate pad is where the conjugated particles are, such as colored latex beads or gold nanoparticles, that are coated with capture molecules, in this case the chimeric protein with the peptides, specific to the target analyte of interest (Yuwei *et al.*, 2021). At last, the nitrocellulose membrane captures molecules immobilized on specific lines or points, forming a test line and sometimes a control line. The test line captures the target analyte or detection tag, while the control line verifies assay functionality (Yuwei *et al.*, 2021).

As well, this test has some crucial steps, like the analyte capture and the formation of the test line.

The analyte capture is when the target analyte, in this case NGAL and transferrin (if present) binds to the chimeric proteins with the peptides, forming a complex of biomarker-chimeric protein.

On the other hand, the formation of the test line is when this complex continues to migrate and reaches the test line, where immobilized capture molecules capture the analyte complex, resulting in the formation of a visible line (Yuwei *et al.*, 2021).

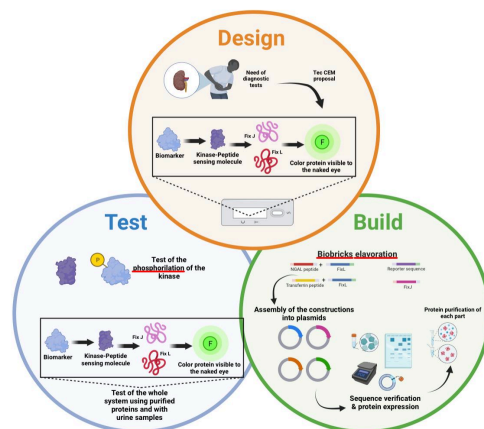


Figure 2. Design-Build-Test cycle, *Design*) Taking into account the need of a diagnostic test, iGEM Tec CEM designed a lateral flow test capable verifications will be needed to then accomplish the purification of each protein component. *Test*) Once the methodology to assemble all of the sequences and purification of the proteins is completed, the idea is also to validate the effectiveness in detecting different concentrations of biomarkers and measuring their interaction with the target. Some next steps are established to facilitate the purification of the proteins and to explore easier paths to sense the phosphorylation and simplify the test.of detecting the biomarkers based on the sensing system of bacteria (Two-component system). *Build*) In order to build the plasmids

needed for the recombinant expression of the chimeric proteins for NGAL peptide and Transferrin peptide, the response regulator and the reporter circuit, a series of assembly

Materials and Methods

- Statistical Analysis for the biomarkers and sensing detection limits

For this specific stage, efforts are directed toward the development of different tests and strategies to contribute to the validation of the proof of concept.

For ensuring the usefulness and specificity of the biomarkers selected (NGAL and transferrin), we started developing a database surrounding several literary works was made to assess the presence of these in early stages of nephropathy, in conjunction with a work made by Xing-Yao Tang *et al.* (2019) where statistical analyses were made to validate the quality of literary studies about these biomarkers. Moreover, molecular docking to iterate and test the binding affinity of our proposed bioreceptors will assess the validity of the peptides from their original source.

The correct folding of the coding protein was simulated with AlphaFold2, specially to ensure that the peptide bioreceptors are exposed and ready to bind to any biomarkers available in the sample solution.

- Molecular Docking

Following the research and design of the detection system, one of the main focuses was to identify peptides that function as bioreceptors of the selected biomarkers. These were obtained from literature, once the sequences of each peptide were identified a PDB file was developed so that a validation could be carried out through molecular docking.

Table 4. Obtained peptide-bioreceptors sequences

Biomarker	Sequence
NGAL (Cho <i>et al.</i> , 2019)	DRWVARDPASIFGGGGSC
Transferrin (Wei <i>et al.</i> , 2020):	CGGGHKYLRW
LFABP (Ku <i>et al.</i> , 2016)	WKIGFXKRLXXVXXXI

The molecular docking process followed a workflow utilizing bioinformatic packages and cm programs (**Figure 3**), as the order follows:

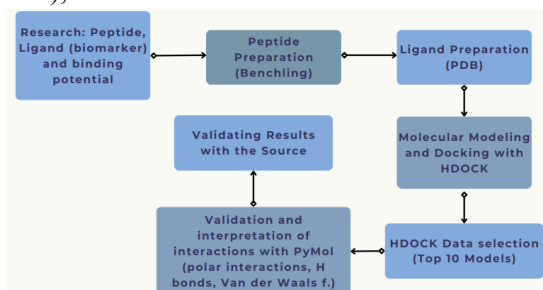


Figure 3. Molecular docking workflow diagram.

- Genetic circuit design

In the development of the design of the genetic circuit for the sensing system, an extensive literature review was conducted to bring support for its distinct components and their specific functionalities, aligning them with the intended functionality. In order to exhibit the main highlights, the subsequent section provides a detailed description of the composition and operation of the proposed sensing system. The sensing system will rely on four key biobricks inspired by *Bradyrhizobium japonicum*, a nitrogen-fixing bacteria on legumes. A two-component regulatory system (TCRS), where the complex FixL-FixJ detects extracellular oxygen (Wright, 2018), extensively explored in research papers for its simplicity and representativeness. This system has been employed for biosensing through synthetic biology, including the creation of a light-sensitive system (Zhang, 2020). FixL (iDLBB_003842), identified as Histidine-Kinase, class I, autonomously senses cytoplasmic oxygen through autophosphorylation, initiating subsequent phosphotransfer reactions to FixJ. FixJ (iDLBB_003843), phosphorylated by activated FixL, binds to the fixK gene promoter, acting as a transcriptional activator within the NarL-like superfamily, ultimately enhancing gene expression for nitrogen fixation under low oxygen concentrations.

Through the replacement of the oxygen-sensing PAS-B domain in *B. Japonicum* with a peptide exhibiting affinity for NGAL and transferrin, a chimeric histidine kinase (HK) denoted as iDLBB_003840 and iDLBB_003841 was engineered, initiating the signal transduction pathway for early nephropathy biomarker diagnostics. The Two-Component Regulatory System (TCRS), designed using FixL-FixJ essentials, delineates into two crucial protein complexes: the "transmitter domain" comprising the HK chimerized with the biomarker-sensitive peptide and the "receiver domain," the response regulator facilitating the transcription of reporter genes upon activation by the transmitter domain (Foussard, 2001).

The whole genetic circuit is structured with distinct components, all which together, adding the biomarkers peptides, conform the proposed sensing system (**Figure 4**):

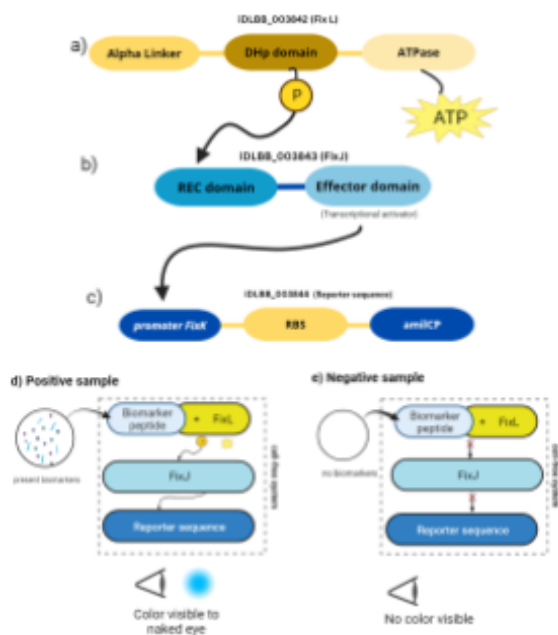


Figure 4: Structure of the main components of the genetic circuit and operation of the sensing system, **a)** iDLBB_003842 (FixL). Taken from BBa_K592004 in iGEM Registry, from 128 to 377 AA, deleting the LOV domain and just keeping its linkers. **b)** iDLBB_003843 (FixJ). The complete sequence was taken from BBa_K592005 in iGEM Registry. **c)** Reporter sequence (iDLBB_003844), complete sequence for promoter FixK taken from BBa_K592006, for RBS BBa_B0030 and for amilCP BBa_K592009 in iGEM Registry. **d)** Positive sample with the visible expression of amilCP. **e)** Negative sample with no visible results.

The function of each component is described in **Table 5**.

Table 5. Description of the functionality of each component of the genetic circuit.

Component	Function
Alpha Linker	Facilitates communication between the sensing domain and the Four-Helix bundle (DHP and ATPase). This linker modulates the autophosphorylation activity of FixL. It propagates conformational changes occurring in the sensing domain to the DHP, inducing structural alterations in the ATP bound to the ATPase.
DHP Domain	It houses the histidine crucial for autophosphorylation; this domain receives the phosphate.
ATPase	It serves as the site where ATP binds and subsequently breaks down, generating a signal from FixL to FixJ. This domain exhibits a conserved structure of several alpha helices grouped over an antiparallel beta sheet, forming a loop that encloses the ATP.
REC domain	Contains an aspartate that receives phosphate from DHP derived from a phosphotransfer reaction, activating the effector domain.
Effector domain (promoter binding)	It has affinity to a DNA sequence (FixK promoter in this case) and acts as a transcriptional activator.
Promoter FixK	A wild-type promoter, to which the phospho-FixJ binds, exhibits considerable leaky activity in the absence of FixJ. The regulation of FixJ is influenced by activated FixL.
RBS (BBa_B0030)	Responsible for facilitating the binding of the ribosome to the plasmid during the translation process.
amilCP	A chromoprotein derived from the coral <i>Acropora millepora</i> , which demonstrates inherent vivid coloration upon expression. Characterized by its distinctive blue/purple hue visible to the naked eye, the protein exhibits maximum absorbance at 588nm, eliminating the necessity for instrumental observation. This intense coloration becomes readily apparent within less than 24 hours of incubation, both in LB and agar culture mediums.

In the case of iDLBB_003840 and iDLBB_003841, although the peptide sequences vary, the FixL part remains consistent. The NGAL binding peptide, with high affinity and specificity for the urinary Neutrophil gelatinase-associated lipocalin (NGAL) biomarker, reported by Cho *et al.* (2019) and expressed in the ER2738 *E. coli* strain. The transferrin peptide, designed by Wei *et al.* (2020) and Santi *et al.* (2017), exhibits high affinity and specificity for transferrin. Its rational design

involves an iterative multiscale-modeling approach coupled with Quantitative Structure-Activity and Relationship analysis and evolutionary algorithms. Standard components were integrated into each biobrick, namely iDLBB_003840, iDLBB_003841, iDLBB_003843, and iDLBB_003844. As illustrated in Figure 5, these biobricks were flanked by a T7 BBa_I719005 promoter specific to T7 RNA polymerase, ensuring robust gene transcription. Subsequently, an RBS (BBa_B0030) for ribosome binding and a lac operator from pET-28a, used for plasmid gene transcription inducible with IPTG, were incorporated. This system interacts with the lacI gene and T7 terminator, which halts transcription and releases T7 RNA polymerase (BBa_K731721).



Figure 5: Design for the expression of Biobricks iDLBB_003840, iDLBB_003841, iDLBB_003843, and iDLBB_003844.

The recombinant expression of both protein complexes, FixL and FixJ, will be optimized for codon usage in *Escherichia coli* (*E. coli*) and subsequently purified for integration into a cell-free system. The reporter circuit, along with the purified FixL and FixJ, will remain latent in the cell-free system until activated by the patient's sample. Upon activation, it initiates the phosphorylation activity of the protein complexes if the relevant biomarkers are present.

- Cloning strategy of the genetic elements of the biosensor elements

In order to express the elements of the biosensor, it is planned to synthesize the sequences (NGAL peptide + FixL, Transferrin peptide + FixL, Reporter sequence, and FixJ) so that each transcriptional unit can then be cloned into its own separate pSB1C3 plasmid. Overlaps will be added to the sequences in the synthesis to favor cloning through Gibson Assembly. Once the fragments have been cloned into the separate pSB1C3 plasmids, *E. coli* transformation will be carried out (either by chemical method or electroporation) to propagate and extract the plasmid for verification.

- Sequence verification

The *E. coli* DH5 α strain will be used for the propagation of the plasmids. Next, Sanger sequencing will be performed to ensure a correct cloning without unexpected mutations. Additional procedures like PCR and restriction enzyme digestion need to be performed as well to verify that the assembly occurs as expected. In regards to the PCR, the *in silico* primer design and the primers'

characteristics are presented in the Results section. As for the restriction enzyme digestion, the *in silico* expected cuts from *EcoRI* and *PstI* are presented in the results section as well. Finally, electrophoresis will verify the plasmid's identity, leading to subcloning of the regions of interest into pET58a expression vectors.

- **Protein Expression**

Once the CDS of interest accomplishes the sequence verification, it will be cut and ligated into an expression plasmid vector, pET58a, which contains a *lac* gene compatible with our *lac* operator for inducing protein expression. The *E. coli* BL21 strain will be used for protein expression and all proteins (as well as the sensing circuit) will be cloned in pET58a for expression. The pET58a plasmids will be cultivated overnight in the LB medium with chloramphenicol at 37°C and 220 rpm until OD 600 reaches 0.6. Afterward, the expression will be induced with various concentrations of IPTG. Following, cells will be harvested by centrifugation at 13000 rpm for 10 min and stored at - 80°C until use.

- **Purification**

Protein purification will be needed in order to get the isolated main parts necessary for our biosensor. Purification of the -His tagged proteins will be performed using High-Affinity Ni-NTA Resin. For purification under native conditions, the collected supernatant will be applied to the Ni-NTA column. After that the column must be washed with the LE buffer containing imidazole, lastly the desired protein will be eluted with the native elution buffer. For purification under denaturing condition, the collected cell pellets may be solubilized in denaturant buffer containing 100 mM NaH₂PO₄, 10 mM Tris-HCl, 8 M urea (pH 8), and incubated for 60 min at room temperature. Subsequently, the mixture may be centrifuged at 12,000 rpm for 30 min to remove any remaining insoluble materials. Afterward, the supernatant will be loaded on the Ni-NTA column, and finally the desired chimeric protein will be eluted with the denaturant buffer containing 250 mM imidazole. All the purification products will be rinsed with a PBS buffer to remove any unwanted reagents. (Soleimani M. *et al.* 2016)

- **SDS-Page**

An 15% SDS-Page gel will be performed in order to verify the expression and separation of the proteins NGAL peptide + FixL, Transferrin peptide + FixL, Reporter sequence, and FixJ, as well a helping determine the correct isolation of those parts once the purifications is performed.

- **Components evaluation of interaction**

Since the basis of FixL-FixJ is phosphorylation, the classic phospho donor for this type of systems is ATP, therefore it is an essential reactive to the experimentation because it provides the phosphate needed to the signaling cascade to activate the transcription of the reporter gene.

All of the methodology described below will be occurring in microtubes before escalating them to the lateral flow assay.

Evaluating the interaction between FixL and FixJ is required. It's necessary to assess the phosphorylation of these proteins using the protocol proposed by Kunzelmann & Webb (2010), in which the generation of ADP is monitored using 5-ATR-ParM, which is used at lower concentrations than that of ADP to generate a fractional saturation of tetramethylrhodamine-ParM, the mechanism of reaction functions. This phosphorylation kinetics of the N-peptide and T-peptide kinases will be measured using 5-ATR-ParM (His6/K33A/D63C/T174A/T175N/ D224C/C287A). Measurements will be carried out in 50 mM Tris·HCl pH 7.5, 80 mM KCl, 5 mM MgCl₂, 2 mM DTT, and 5 M BSA at 20 °C. Reactions are going to be set up with 0.25 M 5-ATR-ParM, 0.005 unit mL⁻¹ of each kinases, the concentrations that may be used are 2 nM of each kinase, 0.5 M ParM and either constant 400 M ATP and varying concentrations of the kinases peptides or constant 300 M kinases peptides and varying ATP. Tetramethylrhodamine fluorescence must be excited at 553 nm and detected at 577 nm. For calibration of the fluorescence signal 0.25 M 5-ATR-ParM was titrated with ADP in the absence of ATP and in the presence of ATP (maximal concentration used). In the range up to 10 M ADP the data could be approximated by a linear dependence. (Kunzelmann, S. *et al.* 2009)

Preliminary Results

Statistical Analysis for the biomarkers and sensing detection limits

A biomarker database was made considering different aspects, such as their concentration in urine, the number of patients, average age, gender, patient's condition (type 1 or 2 diabetes), p value, reported biomarker concentration, albuminuria stage, creatinine concentration (if available), glycosylated hemoglobin percentage, and other observations. After the database was completed, a multivariate analysis was performed using a multiple linear regression model in Excel to find the optimal concentrations of biomarkers in the different stages of the development of diabetic nephropathy, using as reference the amount of urinary albumin and the effective glomerular filtration rate (eGRF). This study showed that NGAL has a mean sensitivity of 82% and a specificity of

81%, and transferrin has a mean sensitivity of 82% and a specificity of 87.7%, for predicting diabetic nephropathy (Tang *et al.*, 2019).

In addition, as mentioned, in the database were investigated the concentrations in urine of these biomarkers in patients with diabetic nephropathy. This investigation was necessary to know the average concentration of these biomarkers in patients, and therefore to know the detection limits of our detection system.

It is reported that the normal concentration of the biomarker NGAL in urine is generally less than 20 nanograms per milliliter. Elevated NGAL levels in urine may indicate acute kidney injury or other renal issues. For this biomarker, the studies reviewed showed that the main criteria for the increase in the concentration of the biomarker in the urine of patients is the age, whether they present any type of albuminuria, and the type of albuminuria they present.

In a study made by Zikry *et al.* (2023), the levels of urinary NGAL were measured in different patients with type 2 diabetes. The results obtained and the characteristics of each group is shown in table 6.

Table 6. Demographics features and anthropometric measures of the study groups and concentrations of urinary NGAL (Zikry *et al.*, 2023).

	Group A (n = 100)		Group B (n = 100)		Group C (n = 100)	
	No.	%	No.	%	No.	%
Sex						
Male	21	21.0	11	11.0	23	23.0
Female	79	79.0	89	89.0	77	77.0
Age (years)						
Min.-Max.	32.0-70.0		38.0-70.0		44.0-70.0	
Mean ± SD.	50.20 ± 10.65		54.34 ± 8.76		58.72 ± 8.02	
Weight (kg)						
Min.-Max.	52.0-138.0		61.0-111.0		47.0-131.0	
Mean ± SD.	82.75 ± 14.67		86.63 ± 12.30		90.39 ± 14.41	
Albuminuria						
	Normoalbuminuria		Microalbuminuria		Macroalbuminuria	
Urinary NGAL (ng/mL)						
Min.-Max.	9.34-20.52		9.88-23.78		11.68-25.28	
Mean ± SD.	14.86 ± 2.54		15.98 ± 3.33		18.33 ± 3.24	

As can be observed in the results of table #, the group of patients with older age and weight that presented a high level of albuminuria (macroalbuminuria) were the ones with the highest concentrations of urinary NGAL, and therefore, the ones with more kidney damage. Nevertheless, another study showed that patients with the same characteristics as group C (table #) had concentrations of urinary NGAL of 352.93 ng/mL approximately (Kaul *et al.*, 2018).

Molecular Docking

Once the selection of the biomarkers was established according to the criteria previously mentioned, the molecular docking was performed in order to determine the interaction of each biomarker and its ligand peptide. The results obtained from the molecular docking HDOCK server scoring system for NGAL, transferrin and the liver fatty acid binding protein (LFABP) were:

Table 7. Results obtained from th HDOCK molecular docking analysis

Biomarker	Residues	Docking score	Confidence score
NGAL	H5-N503, K6-T625, Y7-Y539, R8-S389 and W10-N509, ranging from 1.7 to 3.3 Å.	-266.4 - -212.71	0.91 - 0.77
Transferrin	R6-K124, D7-Q127, S10-T103, G13-T54, G14-R81 and S16-Q28, ranging from 2.6 to 3.6 Å.	-230.9 - -193.07	0.83 - 0.70
LFABP		-105.8 - -93.0	0.29-0.24

*Docking score - -180 to -300: Good affinity/interaction probability. Though the docking score is not recommended to be used as a comparison benchmark.

#Confidence score - 0.5 to 0.7: High affinity/interaction probability. <0.7: Very high affinity/interaction probability. Used as a comparison benchmark.

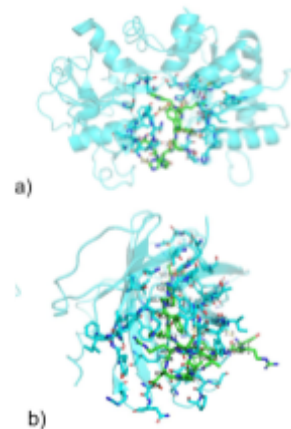


Figure 6. Green: peptide, Blue: biomarker, Red and Blue sticks: active sites; a) Active site and polar interactions of molecular docking model 1 seen with PyMol of serotransferrin and its peptide bioreceptor. b) Active site and polar interactions of molecular docking model 1 seen with NGAL PyMol and its peptide bioreceptor.

Indicating that NGAL and transferrin peptide-bioreceptor have high affinity between these and their respective biomarkers. However, the LFABP peptide-bioreceptor did not show high affinity values for its biomarker and was discarded as a potential biomarker for our project.

The amino acid interactions found in our work coincide with those previously reported by other authors, where the peptide sequences were obtained from. Moreover, such high affinity values were compared with their origin literature studies affinity potentials, where a high affinity

and specificity was reported in such studies for NGAL and transferrin, though LFABP original literature study does not mention the affinity nor specificity level, which contributed to its discardment.

The final AA sequences of the biobricks (iDLBB_003840 - TP_FixL and iDLBB_003841 - NP_FixL) were also modeled to observe their structure (Figure 7 and 8), using PyMol and expecting to see if the peptide (shown in red) is exposed to interact with the biomarker, though few conclusions can be obtained.

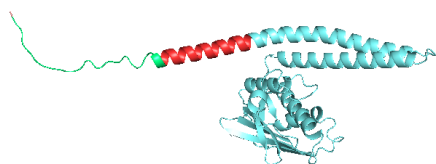


Figure 7. TP_FixL AlphaFold2 structural conformation viewed with PyMol.

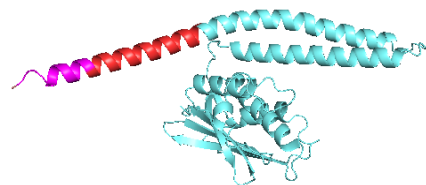


Figure 8. NP_FixL AlphaFold2 structural conformation viewed with PyMol

Genetic Circuit Design

The *in silico* cloning of plasmids yielded the following results: the pSB1C3 plasmid carrying the NGAL peptide-FixL construct had a length of 2981 bp (Figure 9a), while the one with the Transferrin peptide-FixL construct measured 2957 bp (Figure 9b). The plasmid containing FixJ exhibited a size of 1241 bp (Figure 9c), and the total length reached 3174 bp when incorporating the reporter sequence (Figure 9d).

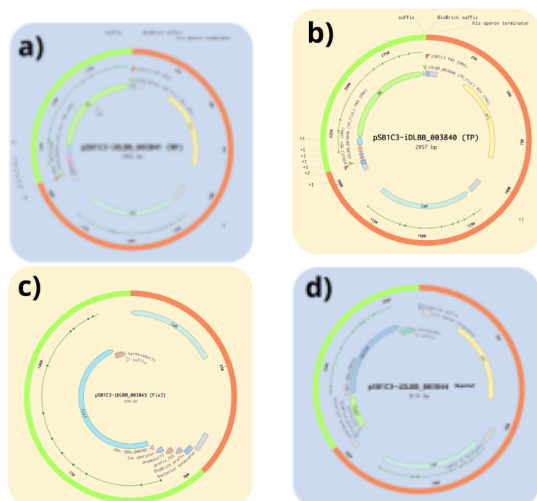


Figure 9. Cloning of the parts of interest into the pSB1C3 plasmid: a) NP-FixJ, b) TP-FixJ, c) FixJ, and d) Reporter sequence.

PCR and cloning

The PCR primers for each part of interest (NP-FixL, TP-FixL, Reporter sequence, and FixJ), were designed *in silico* using Benchling (Figure 10), their main characteristics are shown in Table 7. Then, cloning of each part into a pSB1C3 plasmid was also carried out *in silico*, obtaining the constructions in Figure 10. As can be seen, the constructs contain the genetic elements necessary to promote their expression in a bacterial system. In addition, prefix and suffix sequences compatible with the plasmid pSB1C3 were added. The T7 promoter was selected to be able to control expression using IPTG.

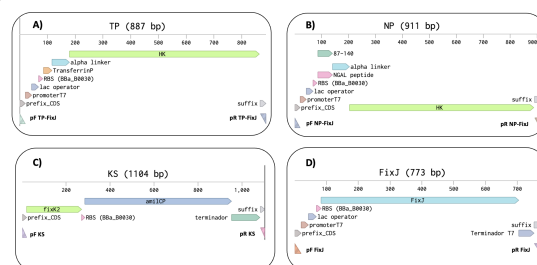


Figure 10. *In silico* primer design for each of the parts: a) NP-FixJ, b) TP-FixJ, c) FixJ, and d) Reporter sequence. [Benchling]

Table 7. Main properties of the PCR primers designed *in silico* [Benchling].

	Sequence	Length (bp)	GC %	Tm (°C)	ΔG homodimer (kcal/mol)	ΔG monomer (kca/mol)	ΔG hairpin (kcal/mol)
forward primers	GAATTCGGCGCC GCTTCTAGa	20	60	58.3	-14.8	-0.5	-0.93
reverse primers	ATGATCATCGCC GGCGACGTC	20	65	61.1	-17.0	-0.5	-1.87

It is important to specify that the PCR product of each part of interest (NP-FixL, TP-FixL, Reporter sequence, and FixJ) was different, being 912 nt, 888 nt, 2070 nt and 774 nt respectively.

With the help of bioinformatics tools such as Benchling we were able to simulate what the cloning of the different sequences of interest would look like. With this, we can use it as a guide for experimental implementation in the future (Figure 10). With this, we can use it as a guide for experimental implementation in the future. With this information we can have a restriction map to simulate and plan digestion, as well as a reference sequence for primer design and sequencing.

Cloning verification through enzymatic digestion

The different genetic constructions that we are going to make in the pSB1C3 vector must be verified to ensure the correct expression of our proteins. For this reason, we made a selection of a couple of enzymes that allow us to evaluate correct cloning. The *in silico* digestion with the expected cuts from *EcoRI* and *PstI* was selected as a verification method to ensure correct cloning (**Figure 11**). In the figure **11**, it can be seen that for each genetic construction a banding pattern is generated that differs from the control and that will demonstrate the correct cloning of the sequence of interest.

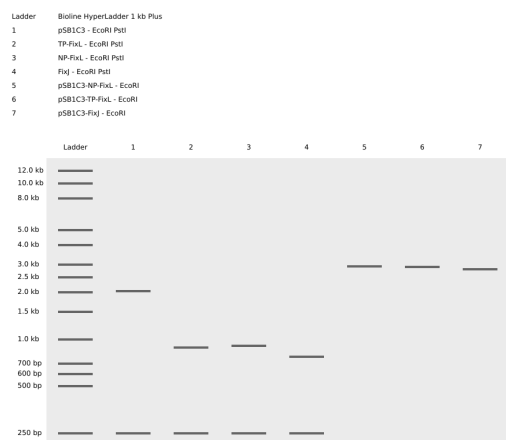


Figure 11. *In silico* digestion of the backbone pSB1C3, the FixL peptide bioreceptors and the final assembled plasmids.

SDS-Page

Once each of the SDS-Page gels are performed either for verifying the expression or the correct purification, for each protein a molecular weight we be expected:

- NP+FixL: 28.87 kDa
- TP+FixL: 28.2 kDa
- FixJ: 22.23 kDa
- Reporter circuit (KS): 3.04 kDa

Component interaction evaluation

The test performed in this part will provide a fluorescent signal, which can be analyzed with a calibration curve and our samples.

The following list of experiments are proposed to validate that our tests verify that the interactions are specific with the biomarker without generating test failures.

- TP-FixL with ATP
- NP-FixL with ATP
- TP-FixL with transferrin with ATP
- TP-FixL with transferrin without ATP
- NP-FixL with NGAL with ATP
- NP-FixL with NGAL without ATP

Posteriorly, when the threshold of detection and verification of the interactions between the proteins are obtained, the system will be assembled, by adding the proteins and the circuit to a cell-free system and expose it to the pure biomarkers and those found in the urine. The samples will then be measured in spectrophotometer at 588 nm as it is the absorbance maximum for the reporter chromoprotein, this allows the quantification of the protein in the sample by following the Beer Lambert law.

For the proteins:

- Characterization of the purified proteins using kinase without peptide as control.
- Evaluation of the activity of FixL-FixJ system on synthetic urine to analyze different pH.

For the whole system:

- Validation of the cell-free system with an already proofed circuit.
- Evaluate the whole system by exposing it to urine with the biomarkers and to the pure protein biomarkers.
- Interaction with chimeric protein with biomarkers at different concentrations and in presence and absence of ATP.

These experiments seek to obtain a broader analysis of how each of the components of the sensing system behave together, in order to determine how they interact both with the pure biomarker and with a sample of it. that is found in the urine, in this way we can identify the sensitivity limits reported by the circuit, as well as analyze its interaction with different inductors.

Conclusions

In conclusion, the purpose of Nefroprot is a point-of-care diagnostic test based on a cell-free system integrated with a genetic circuit to detect the concentrations of significant and specific biomarkers of DN in urine: (N-GAL) and serotransferrin, with the purpose of innovating a simple, accessible and non-invasive alternative diagnostic test for the diagnosis of DN in the early stages. As mentioned previously in the Statistical Analysis for the biomarkers and sensing detection limits, according to the biomarker database, the normal concentration of the NGAL biomarker in urine is generally less than 20 nanograms per milliliter, so, to indicate acute kidney injury or other kidney problems, the expected results are elevated NGAL concentrations. Furthermore, it was shown that the main criterion for the increase in the concentration of the biomarker in the urine of patients is age, whether they present any type of albuminuria, and the type of albuminuria they present; so these are factors to consider when performing the test. Likewise, it is expected to carry out several verification steps such as PCR and restriction enzyme digestion to verify that the assembly

occurs as expected, and finally, through electrophoresis, verify the identity of the plasmid.

Future perspectives

In the context of future perspectives, an honest evaluation of the device's scope reveals identified opportunities for refinement post its initial design. The objective is the evolution toward a quantitative detection system, transcending mere qualitative capabilities. Simultaneously, exploration is underway to assess alternative components involved in signal transduction. Future objectives encompass a Validation Plan for the diagnostic method per NOM-241:2021, contemplating its relevance within the Mexican healthcare landscape. Considerations extend to consulting with experts from the General Health Council to gauge efficiency and efficacy in the context of health economics. Additionally, proposed is the simplification of the sensing system by reducing variables, transforming it into an ATP and dephosphorylation-sensitive system. Consideration of potential alternatives, such as phosphate binding protein or luciferase for phosphate detection, is part of the ongoing evaluation. Furthermore, focus extends to the analysis of peptide interactions with other urinary compounds, contributing to the continuous enhancement of biomarker detection sensitivity and reaction efficiency.

References

Argawal, R. (2021). Pathogenesis of Diabetic Nephropathy. *Chronic Disease and Type 2 Diabetes*. <https://www.ncbi.nlm.nih.gov/books/NBK571720/> doi: 10.2337/db20211-2

Bolignano, D., Lacquaniti, A., Coppolino, G., Donato, V., Fazio, M. R., Nicocia, G., & Buemi, M. (2009). Neutrophil Gelatinase-Associated Lipocalin as an Early Biomarker of Nephropathy in Diabetic Patients. *Kidney and Blood Pressure Research*, 32(2), 91–98. doi:10.1159/000209379

Bosan, I. B. (2007). Recommendations for early diagnosis of chronic kidney disease. *Annals of African Medicine*, 6(3): 130-136. <https://doi.org/10.4103/1596-3519.55719>

Campion, C. G., Sanchez-Ferras, O., & Batchu, S. N. (2017). Potential Role of Serum and Urinary Biomarkers in Diagnosis and Prognosis of Diabetic Nephropathy. *Canadian Journal of Kidney Health and Disease*. 4(1-8). <https://doi.org/10.1177/2054358117705371>

CDC. (2022). Diabetes and Chronic Kidney Disease. *Centers for Disease Control and Prevention*. <https://www.cdc.gov/diabetes/managing/diabetes-kidney-disease.html#:~:text=Both%20type%201%20and%20type%202%20diabetes%20cause%20kidney%20disease.&text=Kidney%20diseases%20are%20the%209th,begin%20treatment%20for%20kidney%20failure>.

Chen, C., Wang, C., Hu, C., Han, Y., Zhao, L., Zhu, X., & Sun, L. (2017). Normoalbuminuric diabetic kidney disease. *Frontiers of Medicine*, 11(3), 310–318. doi:10.1007/s11684-017-0542-7

De los Ríos Castillo, J. L., Sánchez Sosa, J. J., Barrios Santiago, P., & Avila Rojas, T. L. (2005). Calidad de vida en pacientes con nefropatía diabética. *Investigación y Educación en Enfermería*, 23(2): 30-61

Fierro, C. J. A., & Zavala, U. C. (2010). ABC de la nefropatía diabética: una guía práctica para el médico general. *Revista Médica Clínica Las Condes*, 21(4), 579-583.

Fuentes, E., Hernández, Y., López, M. & Berumen, M. (2022). Screening de enfermedad renal crónica en pacientes diabéticos de larga evolución de la UMF (unidad de medicina familiar). *Revista Colombiana de Nefrología*. <http://www.scielo.org.co/pdf/rcnef/v9n1/2500-5006-rcnef-9-01-203.pdf>

Goldstein, S. L. (2011). Acute kidney injury biomarkers: renal angina and the need for a renal troponin I. *BMC Medicine*, 9(1). <https://doi.org/10.1186/1741-7015-9-135>

Hoogeveen, E. K. (2022). The Epidemiology of Diabetic Kidney Disease. *Kidney and dialysis*, 2(3): 433-442. <https://doi.org/10.3390/kidneydial2030038>

Juanola, A., Graupera, I., Elia, C., Piano, S., Solé, C., Carol, M., Pérez-Guasch, M., Bassegoda, O., Escudé, L., Rubió, A. R., Cervera, M., Napoleone, L., Avitabile, E., T. A., Fabrellas, N., Pose, E., Morales-Ruiz, M., Jiménez, W., Torres, F., . . . Ginès, P. (2022). Urinary L-FABP is a promising prognostic biomarker of ACLF and mortality in patients with decompensated cirrhosis. *Journal of Hepatology*, 76(1), 107-114. <https://doi.org/10.1016/j.jhep.2021.08.031>

Kaul, A., Manas Ranjan Behera, M K, Mishra, P., Dharmendra Bhaduarua, Santosh Kumar Yadav, Agarwal, V., Ritu Karoli, Prasad, N., Gupta, A., & Raj Kumar Sharma. (2018). Neutrophil gelatinase-associated lipocalin: As a predictor of early diabetic nephropathy in Type 2 diabetes mellitus. *Indian Journal of Nephrology*, 28(1), 53–53. https://doi.org/10.4103/ijn.ijn_96_17

Kazumi, T. Hozumi, Y. Ishida, Y. Ikeda, K. Kishi, M. Hayakawa, G. Yoshino, Increased urinary transferrin excretion predicts microalbuminuria in patients with type 2 diabetes, *Diabetes Care* 22 (1999) 1176-1180, <https://doi.org/10.2337/diacare.22.7.1176>.

Khalid Al-Rubeaan, Siddiqui, K., Alghonaim, M., Youssef, A. M., Al-Sharqawi, A. H., & Dhekra Alnaqeb. (2017). Assessment of the diagnostic value of different biomarkers in relation to various stages of diabetic nephropathy in type 2 diabetic patients. *Scientific Reports*, 7(1). <https://doi.org/10.1038/s41598-017-02421-9>

Khosla, N., Kalaitzidis, R., Bakris, G. (2010) *Chronic Kidney Disease, Dialysis, and Transplantation (Third Edition)*. <https://doi.org/10.1016/B978-1-4377-0987-2.00004-2>. (<https://www.sciencedirect.com/science/article/pii/B978143770987200042>)

Kunzelmann, S., & Webb, M. R. (2010). A fluorescent, reagentless biosensor for ADP based on tetramethylrhodamine-labeled ParM. *ACS Chemical Biology*, 5(4), 415-425.

Lee, S. Y., & Choi, M. E. (2015). Urinary biomarkers for early diabetic nephropathy: beyond albuminuria. *Pediatric nephrology*, 30, 1063-1075.

Lesley A. Inker, & Andrew S. Levey (2018). 3 - Assessment of Kidney Function in Acute and Chronic Settings. *National Kidney Foundation's Primer on Kidney Diseases* (Seventh Edition), Elsevier, 26-32. <https://doi.org/10.1016/B978-0-323-47794-9.00003-2>

Mizdrak, M., Kumrić, M., Tičinović-Kurir, T., & Božić, J. (2022). Emerging Biomarkers for Early Detection of Chronic Kidney Disease.

Journal of Personalized Medicine, 12(4): 548.
<https://doi.org/10.3390/jpm12040548>

NIH. (2017). Diabetic Kidney Disease. *National Institute of Diabetes and Digestive and Kidney Diseases*.
<https://www.niddk.nih.gov/health-information/diabetes/overview/preventing-problems/diabetic-kidney-disease>

OPS (2021). Diabetes. *Organización Panamericana de la Salud*.
<https://www.paho.org/es/temas/diabetes#:~:text=El%20tratamiento%20de%20la%20diabetes,es%20importante%20para%20evitar%20complicaciones%20A0>

Ogun, A. S., & Adeyinka, A. (2022, November 16). Biochemistry, Transferrin. Nih.gov; StatPearls Publishing.
<https://www.ncbi.nlm.nih.gov/books/NBK532928/>

Reichel, R. R. (2022). Tips on Avoiding Kidney Disease – the 9th Leading Cause of Death in the U.S. *Health Matters*.
<https://healthmatters.wphospital.org/blogs/tips-on-avoiding-kidney-disease-the-9th-leading-cause-of-death-in-the-us/>

Secretaría de Salud. (2022). Diabetes Mellitus Tipo 2 Hospitalaria 2021. *Gobierno de México*.
<https://www.gob.mx/salud/documentos/diabetes-mellitus-tipo-2-hospitalaria-2021>

Shore, N., Khurshid, R. & Saleem, M. (2010). ALPHA-1 MICROGLOBULIN: A MARKER FOR EARLY DETECTION OF TUBULAR DISORDERS IN DIABETIC NEPHROPATHY. University of the Punjab Lahore.
<https://www.ayubmed.edu.pk/JAMC/PAST/22-4/Najla.pdf>

Tang, X., Zhou, J., Luo, F., Han, Y., Zhao, W., Diao, Z., Li, M., Qi, L., & Jy, Y. (2019). Urine NGAL as an early biomarker for diabetic kidney disease: accumulated evidence from observational studies. *Renal Failure*, 41(1), 446–454.
<https://doi.org/10.1080/0886022x.2019.1617736>

Tesch, G. H. (2008). MCP-1/CCL2: A new diagnostic marker and therapeutic target for progressive renal injury in diabetic nephropathy. *American Journal of Physiology-renal Physiology*, 294(4), F697-F701.
<https://doi.org/10.1152/ajprenal.00016.2008>

Thi, T. N. D., Gia, B. N., Thi, H. L. L., Thi, T. N. C., & Huong, P. T. (2019). Evaluation of urinary L-FABP as an early marker for diabetic nephropathy in Type 2 diabetic patients. *Journal of Medical Biochemistry*, 0(0). <https://doi.org/10.2478/jomb-2019-0037>

Soleimani M, Mirmohammad-Sadeghi H, Sadeghi-Aliabadi H, Jahanian-Najafabadi A. Expression and purification of toxic anti-breast cancer p28-NRC chimeric protein. *Adv Biomed Res*. 2016 Apr 19;5:70. doi: 10.4103/2277-9175.180639. PMID: 27169101; PMCID: PMC4854029.

Tang, X., Zhou, J., Luo, F., Han, Y., Zhao, W., Diao, Z., Li, M., Qi, L., & Jy, Y. (2019). Urine NGAL as an early biomarker for diabetic kidney disease: accumulated evidence from observational studies. *Renal Failure*, 41(1), 446–454.
<https://doi.org/10.1080/0886022x.2019.1617736>

Terzic, B., Stanojevic, I., Radojicic, Z., Resan, M., Petrovic, D., Maksic, D., Djekic, J., Ristic, P & Petrovic, M. (2019). Urinary transferrin as an early biomarker of diabetic nephropathy. *VOJNOSANITETSKI PREGLED*.
<https://scindeks-clanci.ceon.rs/data/pdf/0042-8450/2019/0042-84501906615T.pdf>

Thipsawat, S. (2021). Early detection of diabetic nephropathy in patient with type 2 diabetes mellitus: A Review of the literature. *Diabetes and Vascular Disease Research*, 18(6).
<https://doi.org/10.1177/147916412111058856>

Thornton-Snider, J., Sullivan, J., van Eijndhoven, E., Hansen, M. K., Bellosillo, N., Neslusan, C., O'Brien, E., Riley, R., Seabury, S., & Kasiske, B. L. (2019). Lifetime benefits of early detection and treatment of diabetic kidney disease. *PLoS One*, 14(5).
<https://doi.org/10.1371/journal.pone.0217487>

Wright, G. S., Saeki, A., Hikima, T., Nishizono, Y., Hisano, T., Kamaya, M., ... & Sawai, H. (2018). Architecture of the complete oxygen-sensing FixL-FixJ two-component signal transduction system. *Science Signaling*, 11(525), eaaq0825

Varghese, R. T. & Jialal, I. (2023). Diabetic Nephropathy. *StatPearls*.
<https://www.ncbi.nlm.nih.gov/books/NBK534200/>

Villena Pacheco, A. (2021). Factores de riesgo de Nefropatía Diabética. *Acta Médica Peruana*, 38(4), 283-294.

Wu, L., Chiou, C., Chang, P. Y., & Wu, J. T. (2004). Urinary 8-OHdG: a marker of oxidative stress to DNA and a risk factor for cancer, atherosclerosis and diabetes. *Clinica Chimica Acta*, 339(1-2), 1-9.
<https://doi.org/10.1016/j.cccn.2003.09.010>

Yuwei, R., Gao, P., Song, Y., Yang, X. Yang, T., Chen, S., Fu, S., @in, X., Shao, M., Man, C., & Jiang, Y. (2021). An aptamer-exonuclease II (Exo I)-assisted amplification-based lateral flow assay for sensitive detection of *Escherichia coli* 0157:H7 in milk. *Journal of Dairy Science* 104(8), 8517-8529. <https://doi.org/10.3168/jds.2020-19939>

Zhang, P., Yang, J., Cho, E., & Lu, Y. (2020). Bringing light into cell-free expression. *ACS Synthetic Biology*, 9(8), 2144-2153

Zikry, M., Salam, M., & Hay, M. (2023). NGAL (Neutrophil Gelatinase-Associated Lipocalin) as an early biomarker of nephropathy in patients with type 2 diabetes. *Alexandria Journal of Medicine*. <https://doi.org/10.1080/20905068.2023.2230051>